Simulation Optimization of Traffic Light Signal Timings via Perturbation Analysis

William C. Howell
Department of Mathematics
University of Maryland
wch@math.umd.edu

Michael C. Fu
Smith School of Business
Institute for Systems Research
University of Maryland
mfu@isr.umd.edu

July 2, 2006

Abstract

In this paper, we develop a simulation optimization algorithm for determining the traffic light signal timings for an intersection of two one-way street traffic flows modeled as single-server queues. The system performance is estimated via stochastic discrete-event simulation, and gradient-based search based on stochastic approximation is applied. In particular, we use smoothed perturbation analysis to derive both left-hand and right-hand gradient estimators of the queue lengths with respect to the green/red light lengths within a signal cycle. Numerical experiments compare the performance of the gradient estimators with finite-difference estimators and illustrate the optimization algorithm.

Keywords: traffic flow models, traffic control, simulation, perturbation analysis.

1 Introduction

Control of traffic light signal timings is one of the least expensive and most effective means of reducing vehicular congestion in metropolitan road networks (Spall and Chin 1997). This is especially true in times of peak traffic flow, such as during morning and evening rush hours. In this context, a fixed-time red-green cycle is used to most efficiently alternate the flows between competing traffic. These fixed-time cycles are generally based on historical traffic flow data as opposed to current sensor data, which is used for adaptive signal timing control.

In this paper, we consider the problem of determining the optimal fixed-time distribution of the red-green cycle at a single intersection, which has proven to be a challenge for analytical modeling methods (cf. Vogel, Goerick and Seelen 2000; Papageorgiou et. al. 2003). Although coordination *between intersections* is also clearly a critical element in optimizing flow over the *entire* network, our work is intended to serve as a starting point for such a larger goal by introducing a new simulation-based optimization approach.

Many traffic engineering textbooks (e.g., Garber and Hoel 1997; Roess, McShane, and Prassas 2004) prescribe ad hoc heuristic means of setting the red-green cycles based on aggregate traffic flow rates. In the research literature, the problem of efficient traffic flow has been studied and reviewed via many different approaches using optimization methods (e.g., Sen and Head 1997; Schutter and De Moor 1998; Foudladvand, Sandjadi and Shaebani 2004). However, with the notable exception of Spall and Chin (1997), none of these algorithms employ both simulation and optimization. Since most metropolitan traffic planners employ simulation models to aid in traffic flow management, our simulation optimization approach not only advances the state of the art in methodology, but also provides a valuable tool for enhancing traffic flow management.

When considering a single intersection, there are two main fixed-time strategies, stage-based and phase-based. Stage-based strategies determine the optimal split and cycle times. Phase-based strategies take it one step further to determine the optimal stage specifications.

Two of the well-known stage-based fixed-time strategies for a single intersection, SIGSET [1] and SIGCAP [2], were proposed by Allsop in 1971 and 1976, respectively. When given m specified stage specifications, SIGSET and SIGCAP will determine the optimal split and cycle times. SIGSET performs this optimization by deriving capacity constraints and an objective function. The objective function is a nonlinear delay function derived by Webster in 1958 [21]. SIGSET seeks to minimize the total delay. As a result, the optimization problem becomes a linearly constrained nonlinear programming problem. SIGCAP seeks to maximize the intersection's capacity. Slight changes are made to the capacity constraints via the demands. These changes lead to a linear programming problem.

Phase-based fixed-time strategies [13] solve a similar type of problem. The problem addressed in stage-based strategies is extended to consider different staging specifications. These approaches determine split and cycle times, as well as stage specification in order to optimize the total delay or system capacity. The extension of determining stage specifications adds binary variables into the optimization problem, which leads to a binary mixed integer linear programming problem. This type of problem requires an application of a branch-and-bound method that acquire an exact solution. This causes the computation time to be greater than that of the stage-based fixed-time strategies.

Actuated plans use real-time data which is usually provided by detectors that are 40 meters upstream from the intersection. The plan basically employs some form of logic to make decisions on the traffic signal based upon the collected data at these detectors. One of the simplest actuated plans can be explained as follows. The light is kept green for some G_{min} (minimum green light length); if a vehicle is detected, then the light is allowed to stay green for an additional G_{extra} (small increment of time) time. The green light gets G_{extra} additional time until G_{max} (maximum allowable green light length) is reached.

There are more advanced versions of this type of plan, such as the one proposed by Miller in 1963[15], where the decision to change stage is made every T seconds. That is, the plan determines what the time gains and loses, M_k, would be in all directions if the decision to change stage is postponed by $k * T$ seconds, for $k = 1, 2, ...$ seconds. If $M_k < 0$ (i.e., no increase in performance) for all k, then the change is made immediately; otherwise the change is postponed until the next evaluation period.

According to the Federal Highway Administration (FHWA) [4], there is a significant void in signal timing plans, because there is no model designed to provide signal settings for an isolated, actuated intersection. It is possible to use some of the aforementioned plans to deal with this problem; however, the FHWA views this approach as a work-around solution.

Gradient information can be valuable when it comes to system analysis, control and optimization. Of all the approaches reviewed, none make use of gradient information, with the exception of TRANSYT which uses estimated "brute-force" via actual perturbations. In this paper we use gradient information of a more direct nature, namely via perturbation analysis. In fact, to the best of our knowledge, this is the first successful application of perturbation analysis in the traffic signal setting.

Our proposed approach is gradient based, and we derive simulation-based gradient estimators that are more efficient than brute-force finite differences; furthermore, they can be implemented online, which also differentiates the algorithm from that of Spall and Chin [19]. Due to the difficulty of the problem, we apply an approach called smoothed perturbation analysis (SPA), introduced by Gong and Ho [11]. Another simpler technique called infinitesimal perturbation analysis (IPA) is not applicable in this setting [12] because the sample performance measure is discontinuous in the parameter space. Because of this discontinuity, we use the framework of Fu and Hu [8] to derive unbiased left-hand and right-hand gradient estimators for the queue lengths at each of the streets. We then employ these gradient estimators in a stochastic approximation algorithm to optimize the signal light timings. Numerical comparisons with optimization using finite difference estimators illustrate the promise of the proposed approach.

The rest of the paper is organized as follows. In section 2, we lay out the problem setting, including the queueing model and assumptions. In section 3, we provide the detailed derivations of the various SPA estimators, including implementation details and proofs of unbiasedness. In section 4, we report illustrative numerical results on the efficiency of the estimators and their effectiveness in optimizing traffic signal light timings. Finally in section 5, we discuss some conclusions of the work.

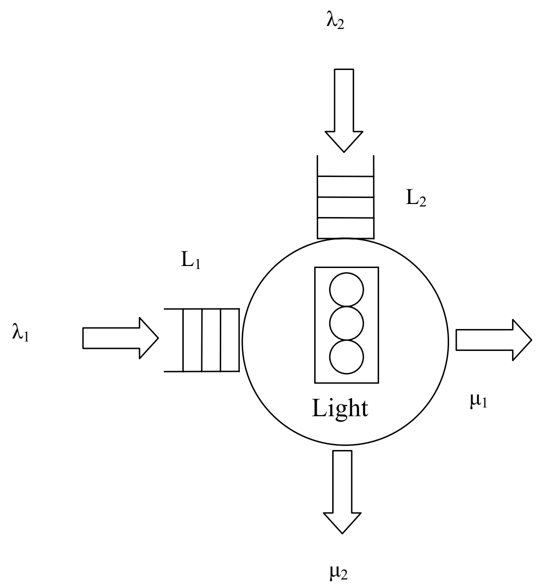

Figure 1: Isolated intersection traffic system visual depiction

2 Problem Setting

The system of interest consists of two one-way streets – labeled 1 and 2 in Figure 1 – intersecting at a traffic light which has two states:

A_1 The light is green for street 1. This state allows both departures and arrivals at street 1, but only arrivals at street 2.

A_2 The light is green for street 2. This state allows both departures and arrivals at street 2, but only arrivals at street 1.

In this model, we ignore yellow light lengths and assume the time to change from one state to another is negligible. The length of a green cycle in states A_1 and A_2 are denoted by T_1 and T_2, respectively. When the light is green for one street, the light is red for the other street. A complete signal cycle is defined by a green-red sequence, and the time to complete such a cycle is denoted by $T = T_1 + T_2$. We assume that the green-red cycle repeats identically and indefinitely, and without loss of generality assume that the sequence begins with a green for street 1. In state $A_j, j = 1, 2$, cars in street j's queue are served one at a time, according to i.i.d. "service times" with mean $1/\mu_j$, c.d.f. F_j and p.d.f. f_j, whereas in the other queue no cars are "served." If a car does not make it through the intersection during a cycle, it must "start over" with a fresh service time during the subsequent green cycle, i.e., the departure process must start over from scratch once it is realized that the car will not exit the queue during the current cycle. Arrivals to each street follow a renewal process with interarrival c.d.f. G_j, asumed to have finite rate λ_j. Unlike the departure process, the arrival processes to both intersection are "on" in both states. The performance measure of interest is the average number of cars waiting at the traffic light for a particular street. By Little's Law, this is essentially equivalent to the average waiting time. We define:

$$\begin{aligned} L_j(t) &= \text{\# cars waiting on street } j \text{ at time } t \ (j = 1, 2); \\ \bar{L}_j(t) &= \text{average queue length for street } j \text{ up to time } t \ = \ \frac{1}{t}\int_0^t L_j(x)dx; \\ N &= \text{\# red-green cycles simulated}; \\ \bar{L} &= \bar{L}_1(NT) + \bar{L}_2(NT). \end{aligned}$$

In other words, the average total queue length performance measure $\bar{L}$ is taken over N green-red cycles. Note that "queue length" throughout includes all cars waiting at the street, even the one currently "in service."

The optimization problem is then given by

$$\min_{T_1, T_2} E[\bar{L}] \tag{1}$$

$$\text{subject to} \quad T_1 + T_2 = T,$$

which we propose to solve by satisfying the first-order condition

$$\nabla_\theta E[\bar{L}] = 0, \tag{2}$$

where θ is the vector of controllable variables (parameters), e.g., T_1 and T_2. To find the value of θ satisfying (2), we use gradient-based simulation optimization via a stochastic approximation recursion of the following form:

$$\theta_{n+1} = \Pi_\Theta \left(\theta_n - a_n \widehat{\nabla} E[\bar{L}(\theta_n)] \right), \tag{3}$$

where a_n is a positive sequence of step sizes, $\widehat{\nabla}$ represents a gradient estimate, and Π_Θ is a projection onto the feasible region Θ.

The gradient estimate in (3) requires estimators for

$$\frac{dE[\bar{L}_j]}{d\theta}, \quad j = 1, 2. \tag{4}$$

We assume T is given, so the constraint essentially reduces (1) to a single-variable optimization problem. With T fixed, a positive perturbation in T_1 results in a negative perturbation in T_2 and vice versa. Although we take T_1 and T_2 as deterministic, a more general formulation could have T_1 and T_2 as random variables, with θ as a parameter in the distribution of T_1 or T_2.

3 Derivation of Estimators

Following the framework of Fu and Hu (1997), the general SPA estimator consists of an infinitesimal perturbation analysis (IPA) term and a conditional term, the latter due to possible critical event order changes, which intuitively are changes in the order of events in a sample path that drastically alter the performance measure of interest. For instance, in our traffic light setting, a perturbation might lead to one less or one more departure in a given green cycle. How to estimate the probability (rate) of such a change and the subsequent expected effect on the performance measure is the key to deriving the SPA estimator.

The general form of the SPA estimator is

$$\left(\frac{dE[\bar{L}_j]}{d\theta}\right)_{SPA} = \frac{d\bar{L}_j}{d\theta} + \lim_{\Delta\theta\to 0} \frac{P_{\mathcal{Z}}(\beta(\Delta\theta))}{\Delta\theta} \lim_{\Delta\theta\to 0} \delta E_{\mathcal{Z}}[\bar{L}_j(\beta(\Delta\theta))], \tag{5}$$

where $\beta(\Delta\theta)$ denotes a critical event change due to a perturbation of $\Delta\theta$, and $\delta E_{\mathcal{Z}}[\bar{L}_j(\beta(\Delta\theta))]$ denotes the corresponding expected change in the performance measure $E_{\mathcal{Z}}[\bar{L}_j]$. The subscript $\mathcal{Z}$ denotes a conditioning on the characterization, which is the set of conditioning quantities on the sample path on which the conditional contribution is estimated, and it will differ for each of the four estimators we derive. In addition to choosing $\mathcal{Z}$, the chief difficulty in implementing an SPA estimator is the estimation of the expected change, $\lim_{\Delta\theta\to 0} \delta E_{\mathcal{Z}}[\bar{L}_j(\beta(\Delta\theta))]$. Ideally, this quantity would be able to be estimated from the original sample path, which we call the nominal path (NP), but its general form is given as $\lim_{\Delta\theta\to 0} \delta E_{\mathcal{Z}}[\bar{L}_j(\beta(\Delta\theta))] = E_{\mathcal{Z}}\left[\bar{L}_j^{PP} - \bar{L}_j^{DNP}\right]$, which is defined by two other sample paths:

- **NP**: nominal path, the original sample path;
- **PP**: perturbed path, limiting version of nominal path on which the critical event change occurs, that is a version of the NP on which the parameter that causes the event change is just big enough to cause the event change;
- **DNP**: degenerate nominal path, limiting version of the nominal path on which no critical event change occurs, that is a version of the NP on which the parameter that causes the event change is just small enough to not cause the event change;

where the superscripts denote the performance measures on the corresponding sample paths. Over N cycles, the estimator (5) becomes

$$\left(\frac{dE[\bar{L}_j]}{d\theta}\right)_{SPA} = \frac{d\bar{L}_j}{d\theta} + \sum_{i=0}^{N} \lim_{\Delta\theta\to 0} \frac{P_{\mathcal{Z}_i}(\beta_i(\Delta\theta))}{\Delta\theta} \lim_{\Delta\theta\to 0} E_{\mathcal{Z}_i}\left[\bar{L}_j^{PP_i} - \bar{L}_j^{DNP_i}\right]. \tag{6}$$

Since the optimization is with respect to T_1, we will take $\theta = T_1$ throughout. We derive four estimators: left-hand ($\Delta\theta \uparrow 0$) and right-hand ($\Delta\theta \downarrow 0$) estimators for each of the two streets, with l and r subscripts denoting left-hand and right-hand estimators, respectively. The critical event changes, $\beta_i(\Delta\theta)$, are quite intuitive: a shortening of a green cycle could cause a departure to be lost during the cycle, whereas a lengthening could allow an additional departure.

3.1 Right-Hand Estimator for Queue 1

We first consider queue 1 with $\Delta\theta > 0$, corresponding to the right-hand estimator for $dE[\bar{L}_1]/d\theta$. In this case ($\Delta\theta = \Delta T_1 > 0$), there is a positive perturbation in the green

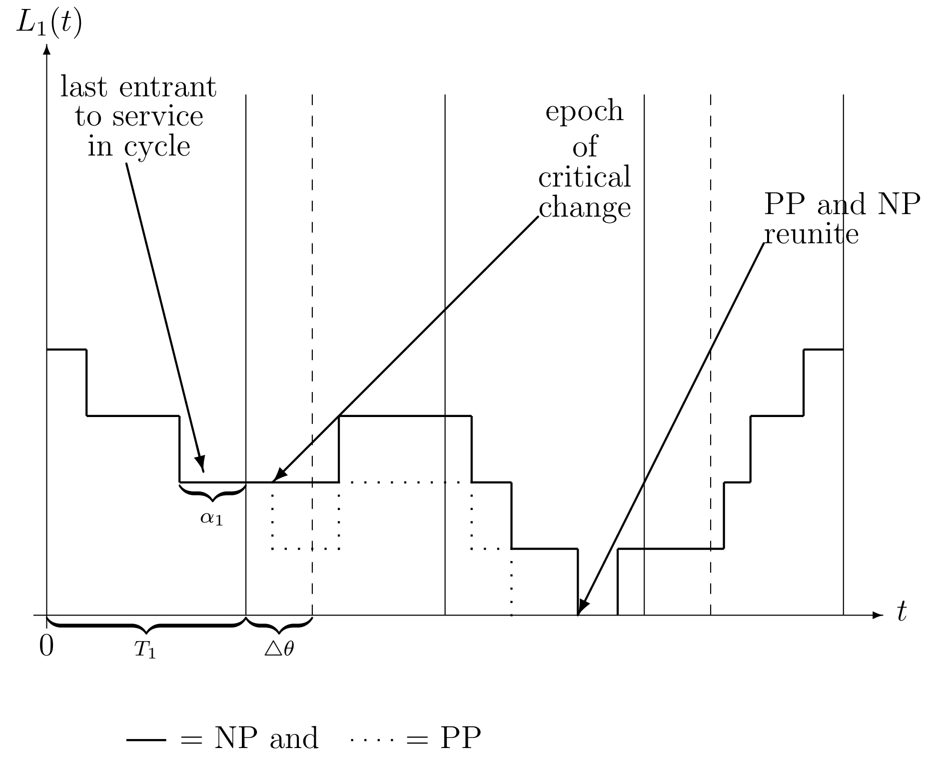

Figure 2: Example of $L_1(t)$ sample path of two-queue vehicular traffic system with positive perturbation of ($\triangle\theta > 0$) T_1 cycle

signal length of street 1 while keeping the total signal cycle length, T, unchanged. Since small perturbations at the end of T_1 do not affect the departure times of cars from street 1, the IPA contribution is zero. A small enough increase in the green signal length would not cause any change in the queue length for street 1; however, a large enough increase would lead to an additional departure; in other words, the performance measure is piecewise constant. The critical change in this case is this additional departure. An additional departure is possible if and only if the queue is nonempty at the light change. When nonempty, the last car to enter service is the only candidate for a critical change, because the probability of more than one critical change is of higher order and can thus be ignored. Thus we only consider the last car as a possible extra departure. To calculate the probability rate and expected effect of this critical change, we condition on all arrivals and service times except for the last entry to service during the current A_1 state. Since the only critical event change in a cycle is a function of the last entry to service, we can index by cycles, and we define:

$$
\begin{aligned}
\alpha_i &= \text{time until light change from last entry of service during } i\text{th cycle,} \\
\mathcal{S} &= \text{set of all service times,} \\
\mathcal{S}_i^* &= \text{last service time of } i\text{th cycle,} \\
\Lambda &= \text{set of all arrival times,} \\
\mathcal{Z}_i &= \mathcal{S}\backslash\{\mathcal{S}_i^*\} \ \cup \ \Lambda,
\end{aligned}
$$

where the service time for the last car to enter service in cycle i is greater than α_i. DNP and PP are then defined by the critical change occurring precisely at the green/red light change, with the service times of the last car to enter service being α_i^+ and α_i^-, respectively. If X denotes a random variable with service time distribution F_1, then the probability of a critical change is given by

$$P(\beta_i(\Delta\theta)) = P(X \leq \alpha_i + \Delta\theta \mid X \geq \alpha_i), \tag{7}$$

and hence

$$\lim_{\Delta\theta\to 0} \frac{P(\beta_i(\Delta\theta))}{\Delta\theta} = \frac{f_1(\alpha_i)}{1-F_1(\alpha_i)}. \tag{8}$$

Thus, the estimator given by (6) becomes

$$\left(\frac{dE[\bar{L}_1]}{d\theta}\right)_{SPA,r} = \frac{1}{NT}\sum_{i=1}^{N} \frac{f_1(\alpha_i)}{1-F_1(\alpha_i)} E_{\mathcal{Z}_i}[\bar{L}_1^{PP_i} - \bar{L}_1^{DNP_i}]. \tag{9}$$

To calculate the resulting expected effect, $E_{\mathcal{Z}}\left[\bar{L}_j^{PP_i} - \bar{L}_j^{DNP_i}\right]$, we observe that starting at the critical change, $L_1^{DNP_i}(t)$ will be identical to $L_1(t)$, whereas $L_1^{PP_i}(t)$ will be one lower than $L_1(t)$ until $L_1(t)$ empties. Thus we have that $L_1^{DNP_i}(t) = L_1^{PP_i}(t) + 1$ for all t from the epoch of the first light change after the critical change to the time when the system first empties after the critical change (see Figure 2 for an example). Figure 2 shows one possible sample path, we note that the last entrant to service that does not exit the system could have also been an arrival to an empty queue. Thus,

$$E_{\mathcal{Z}_i}[\bar{L}_1^{PP_i} - \bar{L}_1^{DNP_i}] = -E[\min(NT, \inf\{t > \tau \mid L_1(t) = 0\})] - \tau, \tag{10}$$

where $\tau = iT - T_2$ corresponds to the epoch of the ith light change from green to red (for street 1). Estimation of (10) can be done offline as follows. We define

$$
\begin{aligned}
\gamma_i &= \text{residual interarrival time at the epoch of the } i\text{th light change,} \\
R_N^{(1)}(\gamma_i) &= \text{expected time to empty queue 1, given } N \text{ cars in the queue} \\
&\quad\ \text{and an initial interarrival time of } \gamma_i, \\
Q_i &= \text{number in queue at the epoch of the } ith \text{ light change from green to red,}
\end{aligned}
$$

and thus (10) is equal to $R_{Q_i}^{(1)}(\gamma_i)$, so the estimator given by (9) becomes

$$\left(\frac{dE[\bar{L}_1]}{d\theta}\right)_{SPA,r} = \frac{1}{NT}\sum_{i=1}^{N} \frac{f_1(\alpha_i)}{1-F_1(\alpha_i)} \left[-R_{Q_i}^{(1)}(\gamma_i)\right]. \tag{11}$$

Note that the sign of the estimator will be negative, which makes intuitive sense, because an increase in the green signal length should decrease the average queue length.

3.2 Right-Hand Estimator for Queue 2

We now consider the case of queue 2 with $\Delta\theta > 0$ to derive the right-hand estimator for $dE[\bar{L}_2]/d\theta$. An increase in T_1 affects the entrance to service of cars in queue 2 and hence the departure times of cars in queue 2, because it results in a decrease in T_2, delaying the transition from state A_1 to A_2 and leading to an IPA perturbation in the departure times of every car in the initiating busy period (IBP) of the cycle. If the queue was empty at the beginning of the green period, we say that the particular cycle has no initiating busy period and hence there will be no IPA contribution for that cycle. Also any car that arrives after an idle period will not be affected by a perturbation in T_1, i.e., once the system empties, the perturbation is lost. The critical change for this case is a loss of a departure. A departure by a car that is in the initiating busy period may be eliminated by the perturbation and hence represents a potential critical change. To calculate the probability rate and expected effect of each of these possible critical changes, we condition on all arrival times and all service times except that of the kth initiating busy period departure of the ith period. We define:

$$\begin{aligned}
\alpha_i^k &= \text{time until light change from the entry to service of the } k\text{th IBP departure,}\\
\mathcal{S}_i^{*k} &= \text{set of all service times of } i\text{th cycle prior to } k\text{th IBP departure,}\\
\mathcal{Z}_i^k &= \mathcal{S}\backslash\{\mathcal{S}_i^{*k}\} \ \cup \ \Lambda,\\
H_i &= \text{number of IBP departures during } i\text{th cycle,}\\
\beta_i^k &= \text{critical change cause by } k\text{th IBP departure during } i\text{th cycle,}\\
PP_i^k &= \text{perturbed path caused by } k\text{th IBP departure during } i\text{th cycle,}\\
DNP_i^k &= \text{degenerate nominal path caused by } k\text{th IBP departure during } i\text{th cycle.}
\end{aligned}$$

If X denotes a random variable with service time distribution F_2, then the probability rate of a critical change is given by

$$\lim_{\Delta\theta\to 0}\frac{P(\beta_i^k(\Delta\theta))}{\Delta\theta} = \lim_{\Delta\theta\to 0}\frac{P(X \geq \alpha_i^k - \Delta\theta \mid X \leq \alpha_i^k)}{\Delta\theta} = \frac{f_2(\alpha_i^k)}{F_2(\alpha_i^k)}. \tag{12}$$

Thus, the estimator given by (5) becomes

$$\left(\frac{dE[\bar{L}_2]}{d\theta}\right)_{SPA,r} = \frac{1}{NT}\left(\sum_{i=1}^{N} H_i + \sum_{i=1}^{N}\sum_{k=1}^{H_i}\frac{f_2(\alpha_i^k)}{F_2(\alpha_i^k)}E_{\mathcal{Z}_i^k}[\bar{L}_2^{PP_i^k} - \bar{L}_2^{DNP_i^k}]\right). \tag{13}$$

Estimation of the expected difference between $\bar{L}_2^{PP_i^k}$ and $\bar{L}_2^{DNP_i^k}$ is similar to the previous estimator. The difference in these two performance measures is the difference in the time it takes for the two paths to empty, which can be estimated by simulating the expected time to empty the system, given that the initial queue length is equal to the queue length of the PP path at the time if the light change. Because arrivals are not affected by the perturbation of T_1, we must consider additional arrivals in the expected difference calculation. Defining

$$\begin{aligned} R_N^{(2)}(\gamma_i) &= \text{expected time to empty queue 2, given } N \text{ cars in the queue} \\ & \text{and an initial interarrival time of } \gamma_i, \\ Y_i^k &= \text{number in queue immediately after the epoch of the } k\text{th IBP departure} \\ & \text{during the } i\text{th cycle}, \\ A_i^k &= \text{number of arrivals between } k\text{th entry to service and next light change} \\ & \text{during } i\text{th cycle}, \end{aligned}$$

the final estimator becomes

$$\left(\frac{dE[\bar{L}_2]}{d\theta}\right)_{SPA,r} = \frac{1}{NT}\sum_{i=1}^{N} H_i + \frac{1}{NT}\sum_{i=1}^{N}\sum_{k=1}^{H_i}\frac{f_2(\alpha_i^k)}{F_2(\alpha_i^k)} R^{(2)}_{Y_i^k + A_i^k}(\gamma_i). \tag{14}$$

The sign of the estimator will be positive, which makes intuitive sense, because a decrease in the green signal length should increase the average queue length.

3.3 Left-Hand Estimator for Queue 1

We now consider the case of queue 1 with $\Delta\theta < 0$ to derive the left-hand estimator for $dE[\bar{L}_1]/d\theta$. Decreasing T_1 affects the departures of cars in queue 1 by advancing the transition from state A_1 to state A_2. Because the perturbation occurs at the end of the cycle, a small enough perturbation will have no effect on the departure times of cars. Therefore, there is no IPA contribution for the estimator. The critical change for this case is again a loss of a departure. Every car that successfully completes service represents a potential critical change. To calculate the probability rate and expected effect of these possible critical changes, we condition on all arrival times and all service times except that of the kth IBP departure. If X denotes a random variable with service time distribution F_1, then the probability rate of a critical change is given by

$$\lim_{\Delta\theta\to 0}\frac{P(\beta_i^k(\Delta\theta))}{\Delta\theta} = \lim_{\Delta\theta\to 0}\frac{P(X \geq \alpha_i^k - \Delta\theta \mid X \leq \alpha_i^k)}{\Delta\theta} = \frac{f_1(\alpha_i^k)}{F_1(\alpha_i^k)}. \tag{15}$$

Thus, the estimator given by (5) becomes

$$\left(\frac{dE[\bar{L}_1]}{d\theta}\right)_{SPA,l} = -\frac{1}{NT}\sum_{i=1}^{N}\sum_{k=1}^{H_i}\frac{f_1(\alpha_i^k)}{F_1(\alpha_i^k)} E_{\mathcal{Z}_i^k}[\bar{L}_1^{PP_i^k} - \bar{L}_1^{DNP_i^k}]. \tag{16}$$

Estimation of the difference between $\bar{L}_1^{PP_i^k}$ and $\bar{L}_1^{DNP_i^k}$ is identical to that in the previous estimator, so the final estimator is given by

$$\left(\frac{dE[\bar{L}_1]}{d\theta}\right)_{SPA,l} = -\frac{1}{NT}\sum_{i=1}^{N}\sum_{k=1}^{H_i}\frac{f_1(\alpha_i^k)}{F_1(\alpha_i^k)} R^{(1)}_{Y_i^k + A_i^k}(\gamma_i). \tag{17}$$

The sign of the estimator will be negative, which makes intuitive sense, because an increase in the green signal length should decrease the average queue length.

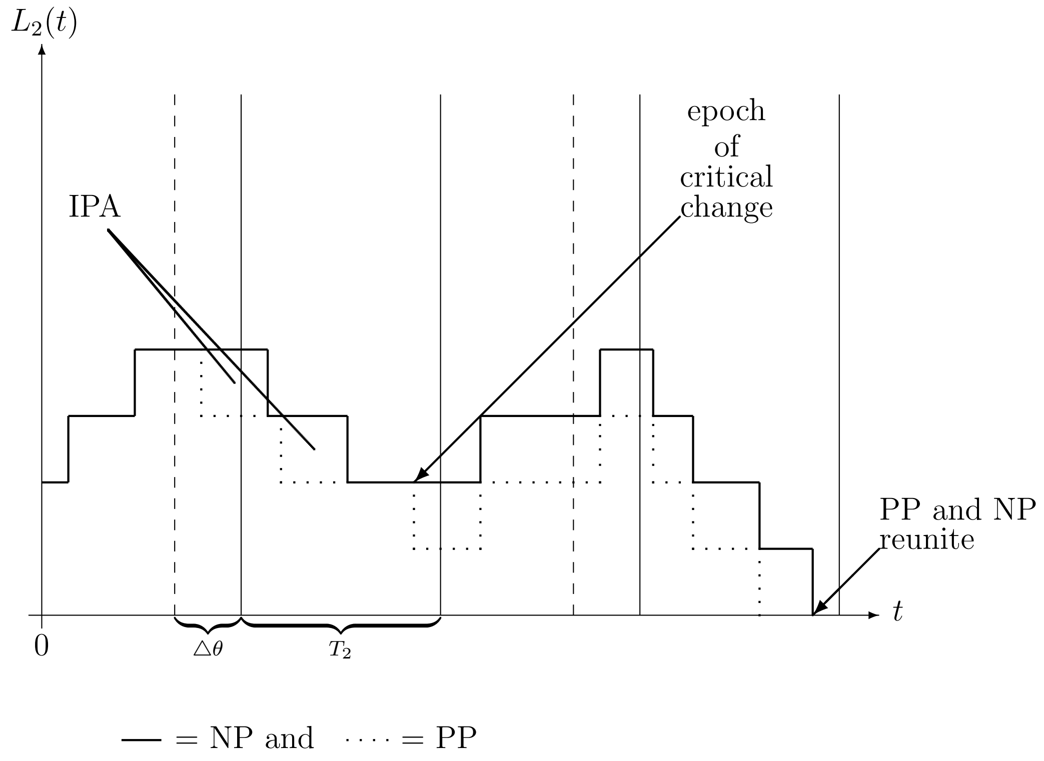

Figure 3: Example of $L_2(t)$ sample path for two-queue vehicular traffic system with negative perturbation of ($\triangle\theta < 0$) T_1 cycle

3.4 Left-Hand Estimator for Queue 2

The case of queue 2 with $\Delta\theta < 0$ for the left-hand estimator for $dE[\bar{L}_2]/d\theta$ is similiar to the right-hand estimator for queue 1, except that there is an IPA component. A decrease in T_1 affects the entrance to service of cars in queue 2 and hence the departure times of cars in queue 2, because it results in an increase in T_2, advancing the transition from state A_1 to A_2 and leading to a perturbation in the departure times of every car in the initiating busy period of the cycle (see Figure 3 for an example). If the queue was empty at the beginning of the green period, there will be no IPA contribution for that cycle, and any car that arrives after an idle period will not be affected by a perturbation in T_1, i.e., once the system empties, the perturbation is lost. Except for a sign change, the rest of the analysis proceeds analogously to that used to derive (11). Thus, the estimator given by (5) becomes

$$\left(\frac{dE[\bar{L}_2]}{d\theta}\right)_{SPA,l} = \frac{1}{NT}\sum_{i=1}^{N} H_i + \frac{1}{NT}\sum_{i=1}^{N} \frac{f_2(\alpha_i)}{1-F_2(\alpha_i)} E_{\mathcal{Z}_i}[\bar{L}_2^{PP_i} - \bar{L}_2^{DNP_i}], \tag{18}$$

and the final estimator is given by

$$\left(\frac{dE[\bar{L}_2]}{d\theta}\right)_{SPA,l} = \frac{1}{NT}\sum_{i=1}^{N} H_i + \frac{1}{NT}\sum_{i=1}^{N} \frac{f_2(\alpha_i)}{1-F_2(\alpha_i)} \left[R_{Q_i}^{(2)}(\gamma_i)\right]. \tag{19}$$

Note that the sign of the estimator will be positive, which makes intuitive sense, because a decrease in the green signal length should increase the average queue length.

3.5 Special Cases

For the special case of exponential interarrival and service times, (11), (14), (17), and (19) respectively simplify to

$$\left(\frac{dE[\bar{L}_1]}{d\theta}\right)_{SPA,r} = -\frac{\mu_1}{NT}\sum_{i=1}^{N} R_{Q_i}^{(1)}, \tag{20}$$

$$\left(\frac{dE[\bar{L}_2]}{d\theta}\right)_{SPA,r} = \frac{1}{NT}\sum_{i=1}^{N} H_i + \frac{\mu_2}{NT}\sum_{i=1}^{N}\sum_{k=1}^{V_i} \frac{R_{Y_i^k+A_i^k}^{(2)}}{e^{\mu_2\alpha_i^k}}, \tag{21}$$

$$\left(\frac{dE[\bar{L}_1]}{d\theta}\right)_{SPA,l} = -\frac{\mu_1}{NT}\sum_{i=1}^{N}\sum_{k=1}^{V_i} \frac{R_{Y_i^k+A_i^k}^{(1)}}{e^{\mu_1\alpha_i^k}}, \tag{22}$$

$$\left(\frac{dE[\bar{L}_2]}{d\theta}\right)_{SPA,l} = \frac{1}{NT}\sum_{i=1}^{N} H_i + \frac{\mu_2}{NT}\sum_{i=1}^{N} R_{Q_i}^{(2)}, \tag{23}$$

where the dependence of $R_N^{(j)}$ on the residual interarrival time has been removed due to the memoryless property of exponential distribution.

3.6 Unbiasedness of the Estimators

The estimators derived in the previous sections are unbiased if

$$E\left[\left(\frac{dE[\bar{L}_j]}{d\theta}\right)_{SPA}\right] = \frac{dE[\bar{L}_j]}{d\theta}, \quad j = 1, 2. \tag{24}$$

To establish (24), some additional conditions are required:

(A1) $F_1(\cdot)$ is Lipschitz continuous with Lipschitz constant K_1.

(A2) $F_2(\cdot)$ is Lipschitz continuous with Lipschitz constant K_2.

We then have the following result.

Proposition 1.

(i) *Under condition (A1), (9) is an unbiased estimator for* $\frac{dE[\bar{L}_1]}{d\theta}$,

(ii) *Under condition (A1), (16) is an unbiased estimator for* $\frac{dE[\bar{L}_1]}{d\theta}$,

(iii) *Under condition (A2), (13) is an unbiased estimator for* $\frac{dE[\bar{L}_2]}{d\theta}$,

(iv) *Under condition (A2), (18) is an unbiased estimator for* $\frac{dE[\bar{L}_2]}{d\theta}$.

estimator	$dE[\bar{L}_1]/d\theta$	$dE[\bar{L}_2]/d\theta$
SPA (RH)	-2.465 (0.001)	2.463 (0.001)
SPA (LH)	-2.465 (0.001)	2.464 (0.001)
FD (.05)	-2.475 (0.024)	2.455 (0.021)

Table 1: Simulation Results for “C1” (standard errors in parentheses)

estimator	$dE[\bar{L}_1]/d\theta$	$dE[\bar{L}_2]/d\theta$
SPA (RH)	-8.303 (0.006)	0.0687 (0.000003)
SPA (LH)	-8.295 (0.007)	0.0687 (0.000003)
FD (.05)	-8.169 (0.115)	0.0687 (0.000035)

Table 2: Simulation Results for “C2” (standard errors in parentheses)

Proof. See appendix A. □

For the special case of F_j $(j = 1, 2)$ exponentially distributed, (A1) and (A2) are automatically satisfied, so we have the following corollary.

Corollary 1. *If G_j and $F_j\,(i = 1, 2)$ are exponential distributions, then (22) and (20) are unbiased estimators for $\frac{dE[\bar{L}_1]}{d\theta}$, and (23) and (21) are unbiased estimators for $\frac{dE[\bar{L}_2]}{d\theta}$.*

4 Numerical Results

We implemented all four SPA estimators and compared them with various symmetric finite difference (FD) estimates for two sets of parameters. We then tested their use in optimization. In all cases, we took the interarrival times and service times to be exponentially distributed, so estimators (20),(21),(22), and (23) were used. The same estimators could be used as an approximation for non-exponential times.

4.1 Gradient Estimation

The first case (“C1”) corresponds to symmetric street flows and signal timings: $\mu_1 = \mu_2 = 2.0; \lambda_1 = \lambda_2 = 4.5; T = 60, T_1 = T_2 = 30$. The second case (“C2”) is an asymmetric system: $\mu_1 = 1.5, \mu_2 = 0.75; \lambda_1 = \lambda_2 = 5.0; T = 110, T_1 = 35, T_2 = 75$. The simulations were carried out for $N = 10,000$ cycles over 10,000 replications. The results are shown in Tables 1 and 2. The calculation of the FD estimators is quite sensitive to the difference value chosen; the best results are reported here, where the number in parentheses following the heading “FD” in the tables indicates the specific difference value. Even so, the SPA estimator is more precise, with a standard error always at least an order of magnitude better, and it is also more stable and computationally efficient. In fact, when $\bar{L}$ is also desired, the FD estimators require (on average) nearly three times as much computation time. The confidence intervals for all estimators overlap for both cases.

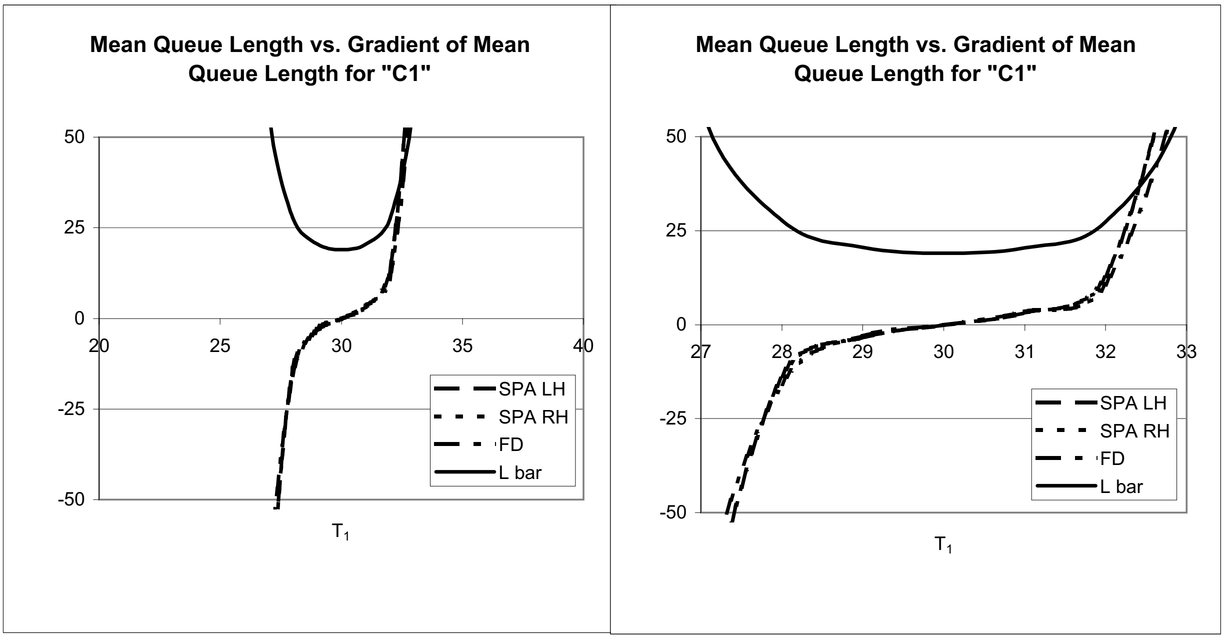

Figure 4: $E[\bar{L}]$ and $\frac{dE[\bar{L}]}{d\theta}$ for "C1"

4.2 Optimization

In the implementation of the SA algorithm (3), we take

$$\Theta = T\left(\frac{\lambda_1}{\mu_1}\right) < T_1 < T\left(1 - \frac{\lambda_2}{\mu_2}\right),$$

which represents the region of stability. We consider cases using the same values for μ_i, λ_i, and T as in section 4.1, where now T_1 will be optimized. Figures 4 and 5 depict the mean and gradient of the average queue length for both the SPA and FD estimators. The mean queue length was obtained via the discrete-event simulation model, in which 10,000 cycles were simulated over 10,000 replications. Because SA is an iterative algorithm, not only are we concerned with reaching the optimum, but we need subsequent updates to not cause deviation from optimum. To this end, we run simulations and count the number of times the average number in system was within p% (for p = 10,5,1) of the minimum average number in system based on the current T_1 from the SA algorithm. We label the three ranges as

- 10%-range : within 10% of the optimal $\bar{L}$;
- 5%-range : within 5% of the optimal $\bar{L}$;
- 1%-range : within 1% of the optimal $\bar{L}$.

All three gradient estimators were implemented, in conjunction with a SA algorithm, for cases "C1" and "C2". Tables 3 and 4 show the number of times each iteration fell within the aforementioned optimum ranges. We also tested the SPA estimators with the

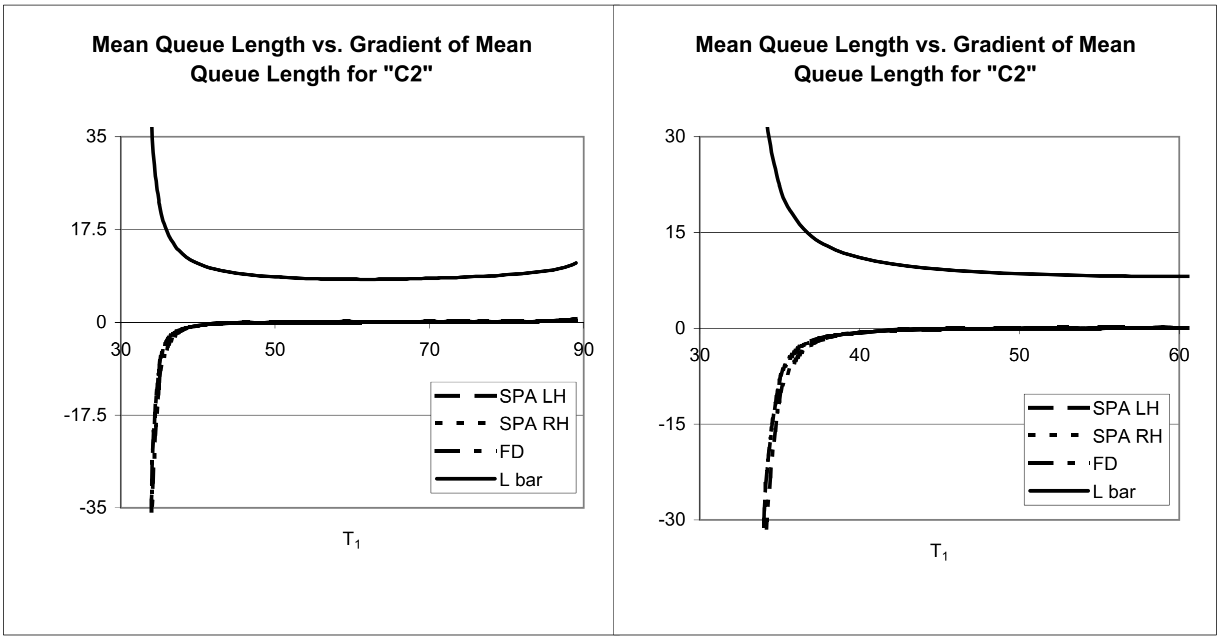

Figure 5: $E[\bar{L}]$ and $\frac{dE[\bar{L}]}{d\theta}$ for "C2"

method	*10%-Range*	*5%-Range*	*1%-Range*
SPA (RH)	77.0 (0.004)	46.4 (0.005)	10.9 (0.003)
SPA (LH)	77.8 (0.004)	45.6 (0.005)	10.9 (0.003)
FD (.05)	76.5 (0.004)	45.0 (0.005)	10.1 (0.003)

Table 3: Mean Number of Times in Optimal Range for "C1" (standard errors in parentheses)

SA algorithm to see if the optimal value was eventually reached. The SA algorithm was allowed to run for 100 iterations to see if the minimum $\bar{L}$ value was reached. This simulation was run for 10 different replications, and these results are shown in Figures 6 and 7. We can see that in each replication, the minimum $\bar{L}$ value was reached relatively quickly, and the estimator never caused a deviation from the minimum for subsequent iterations of the algorithm. These two tests show that the SPA estimators work just as well as FD estimators in iterative gradient descent algorithms such as SA; however, we again mention that FD requires more computational effort.

5 Conclusions

As far as we are aware, this is the first successful attempt to apply direct stochastic gradient estimation techniques to a traffic flow optimization setting. The resulting estimators demonstrated superior computational performance over FD estimators, and in addition can be used on line with real-time traffic updating systems, because unlike FD estimators, they

method	*10%-Range*	*5%-Range*	*1%-Range*
SPA (RH)	92.9 (0.003)	89.9 (0.003)	57.0 (0.005)
SPA (LH)	92.7 (0.003)	90.2 (0.003)	61.0 (0.005)
FD (.05)	94.0 (0.002)	91.8 (0.003)	60.1 (0.005)

Table 4: Mean Number of Times in Optimal Range for "C2" (standard errors in parentheses)

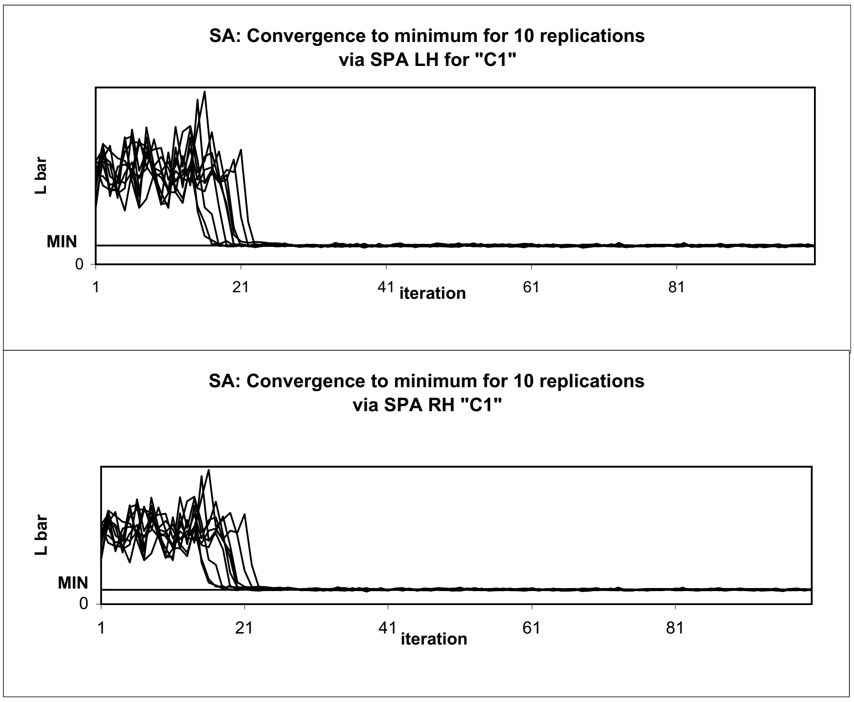

Figure 6: Convergence to minimum for 10 replications of the SA algorithm for "C1" for two different gradient estimation methods: SPA LH SA and SPA RH SA

do not require altering the parameter values. Thus, although we have considered only a single intersection, this work constitutes one important stepping stone in the foundation of simulation-based metropolitan traffic flow management.

A Unbiasedness Proof

We establish (iv) of Proposition 1. The proofs of (i), (ii), and (iii) proceed similarly, and thus their details are omitted here. To proceed, we introduce the following additional notation:

$$\begin{aligned}
\Gamma(NT) &= \{i \leq NT : L_2(iT;\theta) > 0\}; \\
\mathcal{A}_k &= \{L_2(t;\theta) = L_2(t;\theta+\Delta\theta), t = T, 2T, \ldots, kT\}; \\
\mathcal{B}_k &= \{L_2(t;\theta) = L_2(t;\theta+\Delta\theta), t = T, 2T, \ldots, (k-1)T\} \\
&\quad \cup \{L_2(KT;\theta) = L_2(KT;\theta+\Delta\theta)\},
\end{aligned}$$

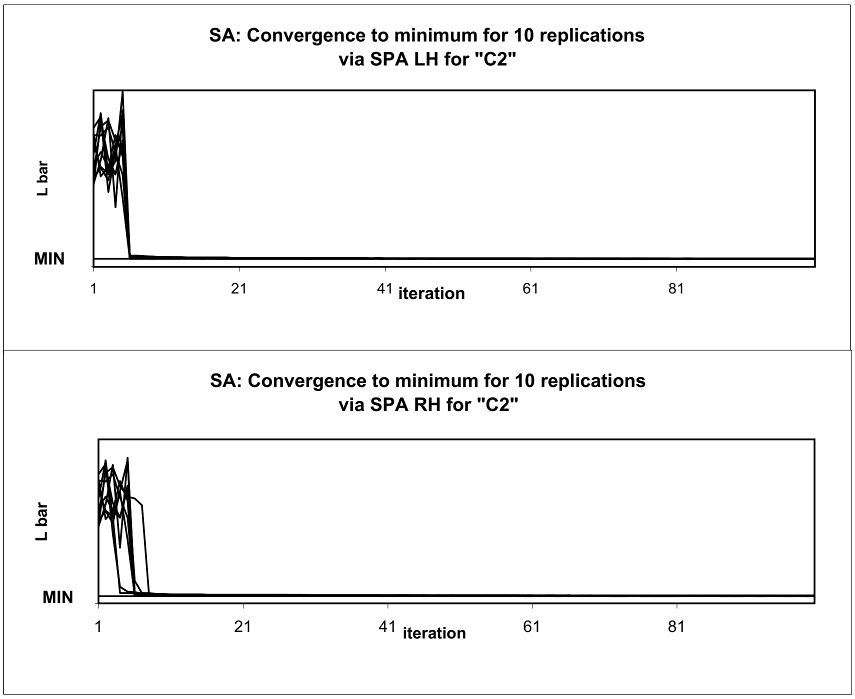

Figure 7: Convergence to minimum for 10 replications of the SA algorithm for "C2" for two different gradient estimation methods: SPA LH SA and SPA RH SA

$k = 1, 2 \ldots, N$, where $\Delta\theta = \Delta T_1 > 0$. The set $\mathcal{Z}_k$ is the characterization for our estimator; it contains everything except the service time of the last entrant to service in period k. $\mathcal{A}_k$ and $\mathcal{B}_k$ are both functions of $\Delta\theta$, though we omit the explicit display of the argument. The event $\mathcal{B}_k$ indicates that a perturbation in the value of θ to $\theta + \Delta\theta$ first causes a change in the queue length in period k. The event $\mathcal{A}_N$ represents the case where the perturbation does not cause a change in the queue length over the entire sample path. Thus $\mathcal{B}_1, \ldots, \mathcal{B}_N, \mathcal{A}_N$ partition our sample space and we can write

$$\frac{dE[\bar{L}_2]}{d\theta} = \lim_{\Delta\theta \to 0} \left\{ \frac{E[(\bar{L}_2(\theta + \Delta\theta) - \bar{L}_2(\theta))\mathbf{1}(\mathcal{A}_n)]}{\Delta\theta} + \sum_{k=1}^{N} \frac{E[(\bar{L}_2(\theta + \Delta\theta) - \bar{L}_2(\theta))\mathbf{1}(\mathcal{B}_k)]}{\Delta\theta} \right\}. \tag{25}$$

We first prove the following lemma.

Lemma 1. *Under condition (A2),*

(a) $E[\bar{L}_2(\theta + \Delta\theta) - \bar{L}_2(\theta))\mathbf{1}(\mathcal{A}_n)] = \Delta\theta \times E\left[\frac{1}{NT}\sum_{i=1}^{N} H_i\right]$.

(b) $\lim_{\Delta\theta \uparrow 0} \frac{E[\bar{L}_2(\theta+\Delta\theta) - \bar{L}_2(\theta))\mathbf{1}(\mathcal{B}_k)]}{\Delta\theta} = E\left[\frac{1}{NT}\frac{f_2(\alpha_k)}{1-F_2(\alpha_k)} R^{(2)}_{Q_k}(\gamma^k)\right]$.

(c) $\lim_{\Delta\theta \downarrow 0} \frac{E[\bar{L}_2(\theta+\Delta\theta) - \bar{L}_2(\theta))\mathbf{1}(\mathcal{B}_k)]}{\Delta\theta} = E\left[\frac{1}{NT}\sum_{i=1}^{V_k} \frac{f_2(\alpha_k^i)}{F_2(\alpha_k^i)} R^{(2)}_{Y_k^i + A_k^i}(\gamma_k)\right]$.

Proof. For part (a), recall that in Section 3.4 we showed

$$(L_2(\theta+\Delta\theta)-L_2(\theta))\mathbf{1}(\mathcal{A}_N) = -\sum_{i=1}^{N} H_i\Delta\theta, \tag{26}$$

which establishes (a).

For part (b), we consider $E[(L_2(\theta+\Delta\theta)-L_2(\theta))\mathbf{1}(\mathcal{B}_k)], k = T, 2T, \ldots, NT$. First we rewrite it as

$$E[E[(L_2(\theta+\Delta\theta)-L_2(\theta))\mathbf{1}(\mathcal{B}_k)|\mathcal{Z}_k]]. \tag{27}$$

We have

$$\begin{aligned}
&|E[L_2(\theta+\Delta\theta)\mathbf{1}(\mathcal{B}_k)|\mathcal{Z}_k]| = \\
&\quad = |E[L_2(\theta+\Delta\theta)|\mathcal{Z}_k, \alpha_k(\theta) < \mathcal{S}_k^* < \alpha_k(\theta+\Delta\theta)]\mathbf{1}(\mathcal{A}_{k-1})P(\alpha_k(\theta) < \mathcal{S}_k^* < \alpha_k(\theta+\Delta\theta))| \\
&\quad = |E[L_2(\theta+\Delta\theta)|\mathcal{Z}_k, \alpha_k(\theta) < \mathcal{S}_k^* < \alpha_k(\theta+\Delta\theta)]\mathbf{1}(\mathcal{A}_{k-1})(F_2(\alpha_k(\theta+\Delta\theta)) - F_2(\alpha_k(\theta)))| \\
&\quad \le K_2\Delta\theta E[L_2(\theta+\Delta\theta)|\mathcal{Z}_k, \alpha_k(\theta) < \mathcal{S}_k^* < \alpha_k(\theta+\Delta\theta)],
\end{aligned}$$

where $\alpha_k(\theta+\Delta\theta) = \alpha_k(\theta)+\Delta\theta$ and the last inequality follows from assumption (A2). To bound the expectation, we introduce notation for a renewal counting process based on the arrivals (without service). Let $\{X_n, n = 1, 2, \ldots\}$ be a sequence of i.i.d. interarrival times with common distribution G_2, and denote the associated counting process $\{P(t), t \ge 0\}$. G_2 generates nonnegative interarrival times with a finite rate (λ_j); thus it follows that $G_2(0) < 1$. Noting that arrivals are independent of θ, from basic renewal theory, we have

$$E\left[\sup_{\Delta\theta} L_2(\theta+\Delta\theta)|\mathcal{Z}_k, \alpha_k(\theta) < \mathcal{S}_k^* < \alpha_k(\theta+\Delta\theta)\right] \;\le\; E[P(NT)] < \infty,$$

so by invoking the dominated convergence theorem (DCT), we have

$$\begin{aligned}
\lim_{\Delta\theta\to 0}\frac{E[\bar{L}_2(\theta+\Delta\theta)\mathbf{1}(\mathcal{B}_k)]}{\Delta\theta} &= E\left[\lim_{\Delta\theta\to 0}\frac{E[\bar{L}_2(\theta+\Delta\theta)\mathbf{1}(\mathcal{B}_k)|\mathcal{Z}_k]}{\Delta\theta}\right] \\
&= E\left[\lim_{\Delta\theta\to 0}\frac{(F_2(\alpha_k(\theta+\Delta\theta)) - F_2(\alpha_k(\theta)))}{\Delta\theta}\right. \\
&\quad \left.\times \lim_{\Delta\theta\to 0} E[\bar{L}_2(\theta+\Delta\theta)|\mathcal{Z}_k, \alpha_k(\theta) < \mathcal{S}_k^* < \alpha_k(\theta+\Delta\theta)]\mathbf{1}(\mathcal{A}_{k-1})\right] \\
&= E[f_2(\alpha_k)E[\bar{L}_2^{PP_k}(t)]] \\
&= E\left[\frac{f_2(\alpha_k)}{1-f_2(\alpha_k)}\mathbf{1}\{\mathcal{S}_k^* > \alpha_k(\theta)\}E[\bar{L}_2^{PP_k}(t)]\right].
\end{aligned}$$

We can similarly show

$$\lim_{\Delta\theta\to 0}\frac{E[\bar{L}_2(\theta)\mathbf{1}(\mathcal{B}_k)]}{\Delta\theta} = E\left[\frac{f_2(\alpha_k)}{1-f_2(\alpha_k)}\mathbf{1}\{\mathcal{S}_k^* > \alpha_k(\theta)\}E[\bar{L}_2^{DNP_k}(t)]\right]. \qquad \square$$

By establishing a bound for each part of our estimator, we are able to use the DCT to make the necessary expectation and limit switch. Thus, combining Lemma 1 with (25) establishes (iv) of Proposition 1. The following lemma and parts (c) and (d) of Lemma 1, needed to establish (i), (ii), and (iii), can be proven analogously, where again $\theta = T_1$.

Lemma 2. *Under condition (A1),*

(a) $E[\bar{L}_1(\theta+\Delta\theta) - \bar{L}_1(\theta))\mathbf{1}(\mathcal{A}_n)] = 0.$

(b) $\lim_{\Delta\theta\downarrow 0} \frac{E[\bar{L}_1(\theta+\Delta\theta)-\bar{L}_1(\theta))\mathbf{1}(\mathcal{B}_k)]}{\Delta\theta} = E\left[\frac{1}{NT}\frac{f_1(\alpha_i)}{1-F_1(\alpha_k)}R^{(1)}_{Q_k}(\gamma_k)\right].$

(c) $\lim_{\Delta\theta\uparrow 0} \frac{E[\bar{L}_1(\theta+\Delta\theta)-\bar{L}_1(\theta))\mathbf{1}(\mathcal{B}_k)]}{\Delta\theta} = E\left[\frac{1}{NT}\sum_{i=1}^{V_k}\frac{f_1(\alpha^i_k)}{F_1(\alpha^i_k)}R^{(1)}_{Y^i_k+A^i_k}(\gamma_k)\right].$

References

[1] R. B. Allsop, "SIGSET: A Computer Program for Calculating Traffic Capcity of Signal-controlled Road Junctions," *Traffic Engineering & Control*, vol.12, pp.58-60, 1971.

[2] R. B. Allsop, "SIGCAP: A Computer Program for Assessing the Traffic Capcity of Signal-controlled Road Junctions," *Traffic Engineering & Control*, vol.17, pp.338-341, 1976.

[3] X.-R. Cao, "Perturbation Analysis of Discrete Event Systems: Concepts, Algorithms, and Applications," *European Journal of Operational Research*, vol.91, 1996, pp.1-13.

[4] Federal Highway Administration Office of Operations,"Signal Timings Process Final Report," 2005.

[5] B. De Schutter and B. Be Moor, "Optimal Traffic Light Control for a Single Intersection," *European Journal on Control*, vol.4, 1998, pp.260-276.

[6] M.E. Fouladvand, Z. Sadjjadi and M.R. Shaebani, "Optimized Traffic Flow at a Single Intersection: Traffic Responsive Signalization," *Journal of Physics A: Mathematical and General*, vol.37, 2004, pp.561-576.

[7] M.C. Fu, "Optimization via Simulation: A Review," *Annals of Operations Research*, vol.53, 1994, pp.199-248.

[8] M.C. Fu and J.Q. Hu, *Conditional Monte Carlo: Gradient Estimation and Optimization Applications*, Kluwer Academic Publishers, Boston, MA; 1997.

[9] M.C. Fu and S.D. Hill "Optimization of Discrete Event Systems via Simultaneous Perturbation Stochastic Approximation," *IEEE Transactions*, vol.29, 1997, pp.233-243.

[10] N. Garber and L.A. Hoel, *Highway and Traffic Engineering (THIRD EDITION)* PWS Pub. Co., Boston, MA; 1997.

[11] W.B. Gong and Y.C. Ho, "Smoothed Perturbation Analysis of Discrete-Event Dynamical Systems," *IEEE Transactions on Automatic Control*, vol.32, 1987, pp.858-867.

[12] L. Head, F.W. Ciarallo, D. Lucas, V. Kaduwela, “A Perturbation Analysis Approach to Traffic Signal Optimization,” INFORMS National Meeting, Washington, D.C., May 5-8, 1996.

[13] G. Improta and G.E. Cantarella, “Control Systems Design for an Individual Signalised Junction,” *Transportation Research B*, Vol.18, pp.147-167, 1984.

[14] A.M. Law and W.D. Kelton, *Simulation Modeling and Analysis*, McGraw-Hill, 3rd edition, 2000.

[15] A. J. Miller, “A Computer Control System for Traffic Networks,” *Proc. 2nd Int. Symp. Traffic Theory*, pp.200-220, 1963.

[16] M. Papageorgiou, C. Diakaki, V. Dinopolou, A. Kotsialos, and Y. Wang, “Review of Road Traffic Control Strategies,” *Proceeding of the IEEE*, vol.91, 2003, pp.2043-2067.

[17] E.S. Prassas, R.P. Roess, and W.R. McShane, *Traffic Engineering*, Prentice Hall, Upper Saddle River, NJ; 2004.

[18] J.C. Spall, “Multivariate Stochastic Approximation Using Simultaneous Perturbation Gradient Approximation,” *IEEE Transactions on Automatic Control*, vol.37, 1992, pp.332-341.

[19] J.C. Spall and D.C. Chin, “Traffic-Responsive Signal Timing for System-Wide Traffic Control,” *Transportation Research - C*, vol.5, 1997, pp.153-163.

[20] A. Vogel, C. Goerick and W. Von Seelen, “Evolutionary Algorithms for Optimizing Traffic Signal Operation,” Proceedings of the European Symposium on Intelligent Techniques (ESIT 2000), Aachen, Germany, pp.83-91, Sept 14-15, 2000.

[21] F.V. Webster, “Traffic Signal Settings,” Road Research Technical Paper No. 39, Research Laboratory, London, UK, 1958.